

See discussions, stats, and author profiles for this publication at: <https://www.researchgate.net/publication/361326680>

# Studying the combined influence of microplastics' intrinsic and extrinsic characteristics on their weathering behavior and heavy metal transport in storm runoff

Article in *Environmental Pollution* · June 2022

DOI: 10.1016/j.envpol.2022.119628

CITATIONS

0

READS

23

2 authors, including:



**Amali Herath**

Mississippi State University

9 PUBLICATIONS 95 CITATIONS

[SEE PROFILE](#)



# Studying the combined influence of microplastics' intrinsic and extrinsic characteristics on their weathering behavior and heavy metal transport in storm runoff<sup>☆</sup>

Amali Herath, Maryam Salehi<sup>\*</sup>

Department of Civil Engineering, The University of Memphis, Memphis, TN, USA

## ARTICLE INFO

### Keywords:

Microplastics  
Photodegradation  
Plastic pollution  
Heavy metals  
Storm runoff

## ABSTRACT

The weathering and contaminant transport behavior of both primary (PMPs) and secondary microplastics (SMPs) are interrelated to their original physiochemical features and variations within the environment. This study examines the influence of PMPs' intrinsic characteristics (polymer structure and crystallinity) and SMPs' extrinsic features (surface oxidation and external sediments attachment) on the photodegradation kinetics, and subsequently Pb(II) and Zn(II) uptake from stormwater. For this purpose, high density polyethylene (HDPE) and low density polyethylene (LDPE) with different degrees of crystallinities were produced as PMPs, and their photodegradation behaviors were compared with original polymers. Furthermore, the SMPs generated by abrasion and surface oxidation of PMPs and the virgin PMPs underwent accelerated photodegradation, and the changes of their crystallinity, surface chemistry, and morphology were examined. Scanning electron microscopy (SEM) imaging and X-ray photoelectron (XPS) studies revealed the formation of cracks and different oxidized functionalities on MPs surface due to UV photodegradation. The vinyl and carbonyl indices calculated using Attenuated Total Reflectance Fourier Transform Infrared (ATR-FTIR) spectroscopy demonstrated an elevated photodegradation rate for SMPs compared to the PMPs. Moreover, the Differential Scanning Colorimetry (DSC) demonstrated an increasing percentage of crystallinity in all MPs due to the photodegradation. The percent crystallinity of HDPE pellets increased after photodegradation from 49.8 to 62.6 and it increased from 17.2 to 38.9 for LDPE pellets respectively. The greater level of increase in crystallinity for LDPE in comparison to HDPE upon photodegradation was referred to as LDPE's greater amorphous content and branched structure. A greater level of metal uptake was obtained for photodegraded LDPE pellets as 2526  $\mu\text{g}/\text{m}^2$  for Pb(II) and 2028  $\mu\text{g}/\text{m}^2$  for Zn(II) respectively.

## 1. Introduction

Global plastic usage has been increased rapidly over the recent decades (Zhang et al., 2021). The estimated worldwide annual plastic production of 367 million tons in 2020 (Statista, 2021) is expected to be doubled within the next twenty years (Huang et al., 2020). A significant portion of the produced plastics may end up in landfills or discard as litter in the environment. The plastic debris can be broken into smaller fragments called macroplastics, microplastics (MPs), and nanoplastics as they are exposed to solar radiation, mechanical, and biological forces (Barbieri et al., 2008; Gong and Xie, 2020; Liu et al., 2020a; Rummel et al., 2017; Webb et al., 2013). The weathering and contaminant

transport behavior of both primary (PMPs) and secondary microplastics (SMPs) could be impacted by their physiochemical features, such as polymeric structure, crystallinity, and surface oxidation during their life cycle, including polymer synthesis, plastic extrusion, usage, and eventually disposal. Thus, it is expected that PMPs and SMPs will have distinct environmental degradation behaviors.

Photodegradation is an important step in initiating the degradation of MPs and is achieved by polymer chain oxidation, chain scission, and crosslinking. Unsaturated bonds and chromophores that present on the polymer chain cause the formation of polymer free radicals via a series of reactions after absorbing UV radiation (Liu et al., 2021). Photodegradation can change the polymer surface chemistry, microstructure,

<sup>☆</sup> This paper has been recommended for acceptance by Baoshan Xing.

<sup>\*</sup> Corresponding author.

E-mail addresses: [msalehiesf@gmail.com](mailto:msalehiesf@gmail.com), [mssfndrn@memphis.edu](mailto:mssfndrn@memphis.edu) (M. Salehi).

mechanical properties, and even the density of MPs floating in water (Zhang et al., 2021). Thus, it may impact the MP's transport behavior and propensity to accumulate contaminants (Holmes et al., 2012). There is still a mismatch between laboratory experiments and actual systems, due to a limited understanding of physiochemical deviations between SMPs and the pristine PMPs. PMPs typically found in laboratory studies are intentionally produced as pellets or beads. By contrast, the SMPs found in field conditions are unintentionally released from plastic litter or PMPs' environmental degradation and have an assortment of heterogeneous shapes, sizes, and even surface oxidized functional groups (Eerkes-Medrano et al., 2015; Meng et al., 2020). The photodegradation behavior of secondary SMPs, which may have heterogeneous surfaces and surface oxidized functional groups, can vary from the PMPs produced as beads or pellets. Addressing this inconsistency will improve the interpretation and validity of the results obtained for polyethylene degradation from environmental studies. Despite the substantive literature dedicated to investigating the role of chemical additives in plastic photodegradation (Barbieri et al., 2008; Rajesh, 2019; Yousif and Hadad, 2013), only limited research is available relating plastic microstructure and surface physio-chemistry to photodegradation kinetics. (Madras et al., 1997; Martínez-Romo et al., 2015; Mateker et al., 2015; Min et al., 2020; Panda et al., 2014). However, the intrinsic polymeric properties such as chemistry, microstructure and extrinsic features, such as surface physio-chemistry alterations or attachment of external objects, could influence the photodegradation of PMPs and SMPs (Bonyadinejad et al., 2022; Min et al., 2020). To date, there is minimal available information connecting the fate of MPs to their primary characteristics. Indeed, understanding this critical interconnection could assist the global community in combating plastic pollution by redesigning plastic products and developing more informed interventions.

The MPs themselves are not the only problem; rather, MPs can leach toxic chemicals and adsorb other contaminants (Devriese et al., 2017; Ma et al., 2016). Due to unique surface properties such as its porosity, high surface area, and various surface functionalities, MPs are very susceptible to adsorb toxic contaminants from aquatic systems. Weathering and aging of MPs in stormwater runoff have increased heavy metal accumulation and this has made an impact on the environment as MPs could serve as a vehicle to transport toxic metals in the aquatic environment (Turner and Holmes, 2015; Wang et al., 2020). The chemical and physical changes caused by the environmental degradation of plastics may alter the contaminant transport behavior by MPs (Aghilinasrollahabadi et al., 2021; Ahamed et al., 2020). A significant portion of plastic pollutants in urban areas and roads could be transported through storm runoff to the adjacent water resources (Kalčíková et al., 2017; Ma et al., 2016). In recent literature, unlike plastic pollutants within the marine and freshwater environment (Gallo et al., 2018; Wang et al., 2019), the degradation of MPs within the urban environment has received scant attention despite its crucial impact on MP contaminant transport behavior. The relative importance of MPs that are delivered by urban stormwater runoff to freshwater resources is poorly understood, limiting the development of efficient management practices.

This study aims to elucidate the influence of intrinsic (polymeric structure, crystallinity) and extrinsic factors (surface oxidation and sediment attachment) on the photodegradation behavior of PMPs and SMPs. The LDPE and HDPE plastics were selected to distinguish the role of the branched polymeric structure of LDPE versus the linear structure of HDPE on MPs' photodegradation kinetics and heavy metal uptake behavior. The PMPs of different degrees of crystallinity were produced and, along with the SMPs generated by sediment abrasion process, were subjected to the photodegradation. The kinetics of Pb(II) and Zn(II) adsorption by LDPE and HDPE PMPs was studied. This study underscores the interrelation among plastics manufacturing and end-of-life processes that control MP fate and contaminant transport within the environment.

## 2. Experimental

### 2.1. Materials and methods

The HDPE and LDPE were selected for this study due to their widespread usage in industries and daily life (Gidigbi et al., 2020). HDPE and LDPE, in the form of pellets, were purchased from Sigma Aldrich with melt indices of 2.2 and 25 g/10 min, respectively. The pellets images and their size distribution are shown in Fig.S1. The Pb(II) and Zn(II) ICP-MS standards (1000 mg/L in 3% nitric acid) were purchased from RICCA chemical company. Water treated with Ultrapure Milli-Q (18 MΩ\*cm) was used for all the experiments.

### 2.2. Generation of PMPs and SMPs with distinct characteristics

- (A) **PMPs of different crystallinity:** Plastic filaments with different percent of crystallinities were produced from new LDPE and HDPE pellets. For this purpose, the HDPE and LDPE pellets were melt-processed using a benchtop filament extruder (Filastruder) at 180 °C and 150 °C, respectively. The plastic filaments were extruded with an annular 3 mm die. A post-drawing apparatus was used to apply two different degrees of tension to the extruded filaments as shown in Fig. S2. Filaments generated at slow and fast post drawing velocities were extruded at a rate of 90 and 330 cm min<sup>-1</sup> respectively. Then all these filaments were cut into 5 mm fragments to represent the microplastics (MPs).
- (B) **SMPs with oxidized surface functions and surface attached sediments:** Unlike MPs found within the aquatic environment, the MPs released to the urban environment may interact with the sediments present in road deposits. Thus, in this study we have simulated the interaction of MPs with urban sediments through shaking the LDPE and HDPE pellets in a mixture of silty sand that contains silt (60%, d < 63 μm), and sand (40%, 63 < d < 500 μm) in amber color bottles for 3 weeks using an orbital shaker at 200 rpm to attach the sediments on their surface and their surface morphology. The sand particles were pyrolyzed at 500 °C for 4 h in a furnace before treating with MPs. The generated SMPs were separated from the sand particles by rinsing with water and ultrasonication for 15 min followed by drying at room temperature for 24 h. To generate surface oxidized functional groups, these HDPE and LDPE pellets were placed in an open glass petri dish and exposed for UV-B radiation using Q-UV Accelerated weathering tester (The Q-panel Company, Cleveland, OH, USA) at a constant intensity of 1.25 mW cm<sup>-2</sup> for 5 weeks at 50 °C. Surface characterization of SMPs was analyzed by Attenuated Total Reflectance Fourier Transformed Infrared Spectrometer (ATR-FTIR) and by Field Emission Scanning Electron Microscopy (FE-SEM).

### 2.3. UVB exposure of PMPs and SMPs

In this study the accelerated photodegradation of both PMPs and SMPs was conducted through UV-B radiation. The UV-B radiation occurs at the wavelength of 285 nm and has sufficient energy to decompose the C-C and C-H functions in PE with the bonding energy of 300 kJ/mol. The polymer structure and degree of crystallinity were considered as intrinsic factors that may influence the photodegradation behavior of MPs. Thus, HDPE and LDPE pellets were selected to identify the influence of linear versus branched polymer structure. Furthermore, the HDPE and LDPE filaments (PMPs) were produced with two degrees of crystallinities, and they were cut into 5 mm fragments and used for photodegradation study. The influence of extrinsic factors such as surface oxidation and surface attached sediments on photodegradation behavior were examined using the new HDPE, LDPE pellets and the generated SMPs. The MPs were placed in glass petri dishes separately and placed in the UV weathering tester at a constant intensity of 1.25

mW cm<sup>-2</sup> with irradiation wavelengths of 280–315 nm (UVB) for 8 weeks at 50 °C. The samples were randomly mixed for every four days to expose the MP surfaces uniformly to UV irradiation.

The information regarding the characterization of plastics' surface morphology and chemistry are provided in the supplementary file.

### 3. Results and discussion

#### 3.1. Intrinsic factors influence the photodegradation of PMPs

##### 3.1.1. Characterization of PMPs

In this study, the photodegradation behavior of HDPE MPs as a linear polymer with a low degree of branching was compared to the LDPE MPs with the branched polymeric structure. The melt indices for HDPE and LDPE were 2.2 and 25 g/10 min respectively, as reported by the supplier. This index shows the weight of melt in grams flowing through the capillary in 10 min. The greater melt index of LDPE compared to the HDPE shows its lower viscosity and subsequently a lower molecular weight compared to the HDPE. Furthermore, the photodegradation behaviors of HDPE and LDPE PMPs with different degrees of crystallinities were compared (Fig. S3). The MP's crystallinity is a critical factor that determines their susceptibility to the fragmentation, photodegradation, and contaminant transport. Polyethylene is a semicrystalline polymer that contains small crystalline regions embedded in large amorphous regions. Length of branching and degree of stereoregularity affect the formation of crystalline areas in the polymer (Ainali et al., 2021). DSC measurements revealed the crystallinity of new HDPE and LDPE pellets as 49.8% and 17.2%, respectively. The data for temperature profiles of HDPE and LDPE are tabulated in Tables S1 and S2. The elevated initial crystallinity of new HDPE compared to LDPE is due to the linear arrangement of monomers within the polymer backbone and the presence of more crystalline zones in the amorphous region. For both HDPE and LDPE filaments, the increased post drawing velocity improved the molecular orientation and enhanced the crystallinity. The crystallinity of new HDPE filaments (PMPs) produced at slow and fast post drawing velocities was found as 51.3% and 52.9% and it was found as 20.5% and 23.4% for new LDPE filaments (PMPs), respectively. Both plastics extruded at slow and fast velocities exhibited more crystallinity than the pellet form. The filaments extruded at the elevated velocity have smaller diameters than the ones extruded at the lower velocity. This leads to packing and arranging the monomers in a more compact and ordered fashion with more crystalline zones. It is reported that high crystalline fraction and orientation in polymers lower the free volume and mobility of the chain segments in the amorphous regions thus making a stabilizing effect upon UV irradiation (Abbasi Mahmoodabadi et al., 2018; Shimada et al., 1988). Upon increasing the duration of UVB exposure, the percent crystallinity increased in all HDPE and LDPE MPs regardless of their form and shape, but this was prominent in LDPE as shown in Table S2. Crystallinity increases when reducing the molecular size and increasing the chain mobility. Besides that, the change in crystallinity is affected by the formation of impurities and reduction in molecular weight but the latter dominates over the formation of irregularities at the first stage of UV exposure. This increases chain scission and enhances the crystallinity (Rabello and White, 1997a; Sun et al., 2020). The initial % crystallinity of HDPE pellets (49.8), filaments extruded under slow (51.3), and fast (52.9) velocities increased up to 62.6, 65.4, and 68.4 after seven weeks of UVB exposure and then dropped in the last week. Chemi-crystallization process took place by crystallizing the degraded freed molecular segments enhanced the overall crystallinity (Carrasco et al., 2001). A decline in the degree of crystallinity in HDPE after the seventh week may be due to the decrystallization process that took place when increasing the time exposed to UV irradiation. It is reported that the generation of carbonyl and hydroperoxides during the photodegradation decrease the molecular regularity and reduce the secondary crystallization. Percent crystallinity of LDPE increased progressively when increasing the radiation duration. The initial % crystallinity of

pellets (17.2), filaments extruded under slow (20.5), and fast (23.4) velocities increased after eight weeks of UV exposure up to 39.0, 41.5, and 48.8, respectively. The increase in % crystallinity was greater in LDPE compared to HDPE and this was due to high radical mobility attained due to less molecular orientation (Rabello and White, 1997b). Filaments extruded at a fast velocity in both HDPE and LDPE exhibited greater crystallinity due to the high molecular orientation obtained by post drawing velocities accordingly. The formation of tertiary radicals is more pronounced in LDPE than HDPE during UV irradiation. Besides that, a greater amorphous fraction of LDPE preferentially renders it to be more susceptible to crosslinking and oxidative degradation due to high oxygen permeability. Additionally, it is reported to have the reactive oxygen species (ROS) formation during the UV exposure which enhances the carbon bond breakage in the polymer and causes the rearrangement of the amorphous fraction (Duan et al., 2022). This made LDPE less thermal resistant than HDPE. It is reported that oxidative reactions increase the surface free energy of the crystals and as a consequence, the peak melting temperature of DSC endotherms shifts to a lower value, and this was observed in both HDPE and LDPE after photodegradation (Fig. 1) (Gulmine et al., 2003; Rabello and White, 1997a). These peaks got narrow and intense due to changes in crystallite sizes and molecular weight differences made by chain scission and secondary crystallization (Fechine and Demarquette, 2008).

##### 3.1.2. Surface chemistry variation of PMPs due to the photodegradation

**(A) ATR-FTIR analysis:** ATR-FTIR spectroscopy was employed to evaluate the chemical changes that occurred upon UVB exposure of HDPE and LDPE PMPs with different degrees of crystallinity. Fig. 2a represents the functional groups present on both HDPE and LDPE pellets in their primary forms before and after UVB exposure. The ATR-FTIR spectra for the PMPs used as filaments in two different degrees of crystallinity are shown in Fig. S4. In primary MPs of HDPE and LDPE, a strong doublet is present at 2918 and 2853 cm<sup>-1</sup> for -CH<sub>2</sub> asymmetrical and symmetrical stretching vibrations, respectively, and the intensities of the peaks are comparatively low in secondary MPs. CH<sub>2</sub> bending deformation band occurs at 1468 cm<sup>-1</sup> and CH<sub>2</sub> rocking deformation band is present at 718 cm<sup>-1</sup>. These peak values match well with the reported literature (Ainali et al., 2021; D'Amelia et al., 2016). Upon UV photodegradation a major peak appeared in the carbonyl region (1786-1698 cm<sup>-1</sup>) for both HDPE and LDPE MPs corresponding to the various oxidized products including carboxylic acids, ketones, aldehydes, and lactones (Chiellini et al., 2006; Suresh et al., 2011). Additionally, a broad peak appeared in 1162 cm<sup>-1</sup> for the C-O groups, and this was more prominent in photodegraded LDPE than HDPE (Benítez et al., 2013).

The photodegradation process of PE was outlined by quantitative analysis of carbonyl, vinyl, and hydroxyl indices as shown in Fig. 3. Carbonyl index ( $I_{CO} = A_{1712}/A_{2866}$ ) was calculated by the ratio of FTIR absorbance at 1712 cm<sup>-1</sup>, stretching vibration of the carbonyl group (C=O), and the IR absorbance at 2866 cm<sup>-1</sup> as the reference value. Vinyl index ( $I_V = A_{909}/A_{1866}$ ) was calculated by the ratio of FTIR absorbance at 909 cm<sup>-1</sup>, stretching vibration of the vinyl group (CH<sub>2</sub>=CH), and the IR absorbance at 2866 cm<sup>-1</sup> as the reference value. Hydroxyl index ( $I_{OH} = A_{3300}/A_{2866}$ ) was calculated by the ratio of FTIR absorbance at 3300 cm<sup>-1</sup>, stretching vibration of the hydroxyl group (-OH), and the IR absorbance at 2866 cm<sup>-1</sup> as the reference value. In the present study absorbance at 2866 cm<sup>-1</sup> was used as the reference value for calculating these indices since this band remained constant throughout the photodegradation study (Ainali et al., 2021; Babaghayou et al., 2016; Martínez et al., 2021). The absorbance value selected as 2866 cm<sup>-1</sup> for reference is the valley obtained between the doublet which corresponding to -CH<sub>2</sub> asymmetrical and symmetrical stretching vibrations at 2918 and 2853 cm<sup>-1</sup>, respectively. (Babaghayou et al., 2016). Carbonyl index for primary HDPE and LDPE (pellets and filaments in different degrees of chain orientation) increased upon increasing the time exposed to the UV radiation. The carbonyl index of

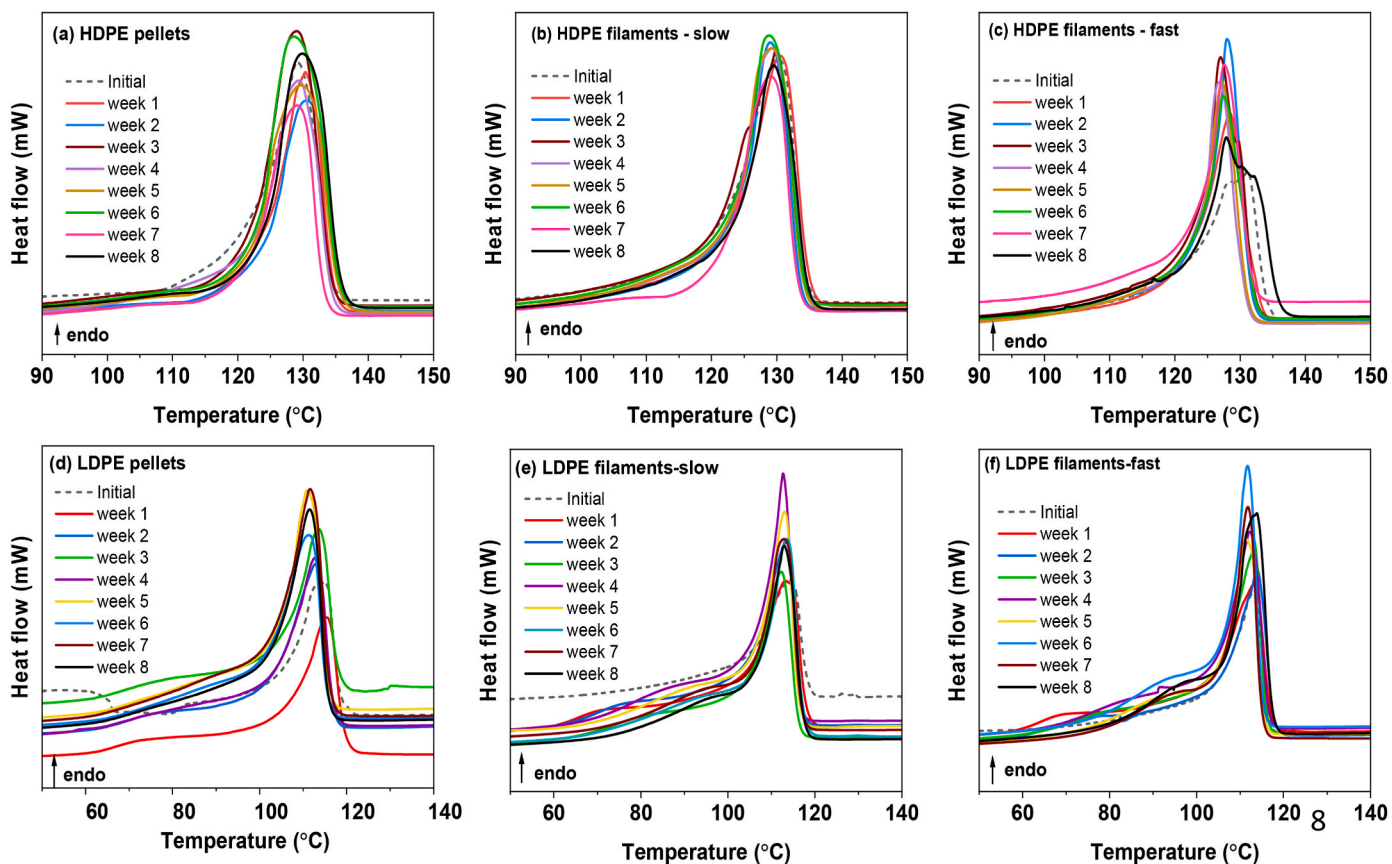


Fig. 1. Endotherm graphs for primary HDPE and LDPE.

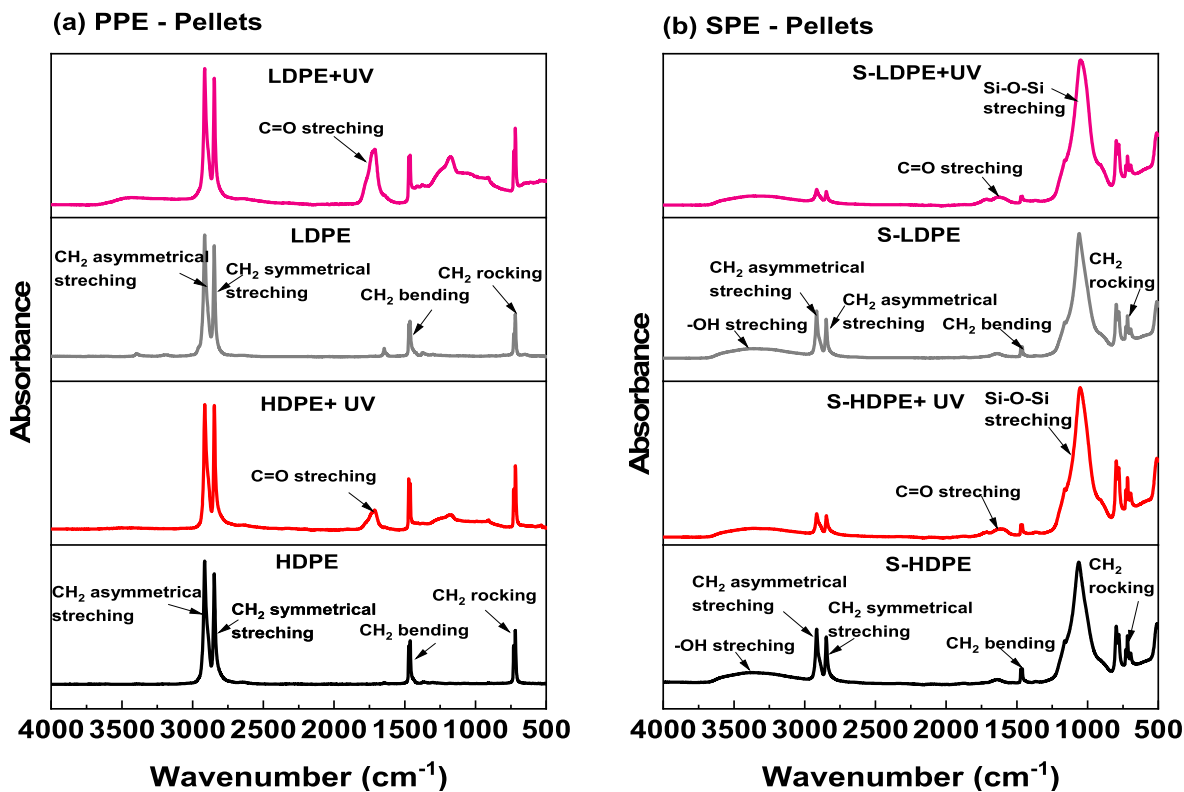
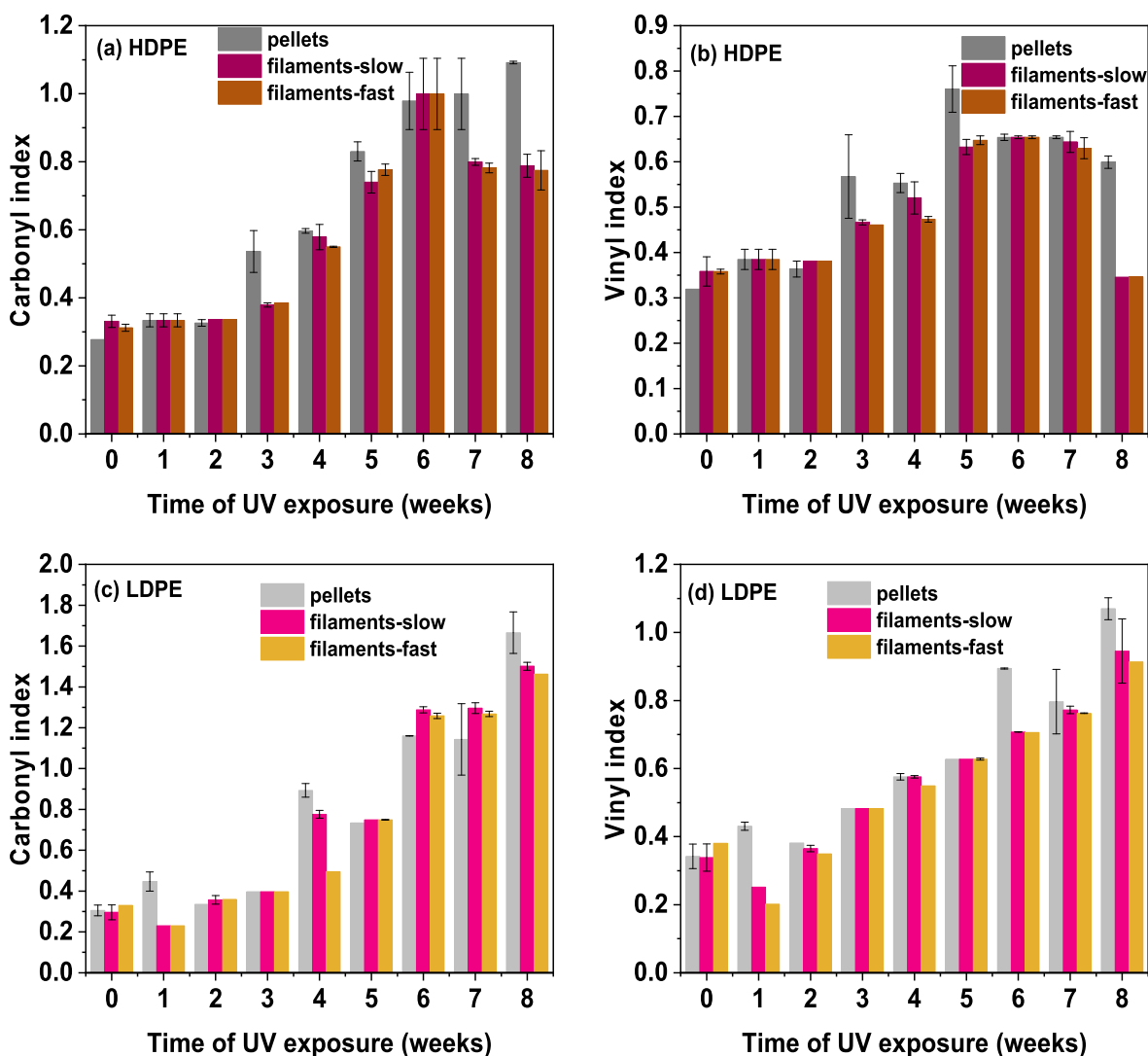


Fig. 2. ATR-FTIR spectra for (a) primary HDPE and LDPE pellets (PPE) before and after UV photodegradation for eight weeks. (b) secondary HDPE and LDPE pellets (SPE) before and after UV photodegradation for five weeks.



**Fig. 3.** Carbonyl and vinyl indices for MPs produced as pellets and filaments with different chain orientations (slow and fast) (a), (b) HDPE and (c), (d) LDPE after exposure to UV degradation. Error bars are from the standard deviation from three replicates.

HDPE pellets increased up to 1.05 after exposing eight weeks to UV radiation (Fig. 3a). Filaments generated at slow and fast velocities exhibited high  $I_{CO}$  up to seven weeks and dropped in the last week. Nevertheless,  $I_{CO}$  of all types of LDPEs increased progressively when increasing the irradiation duration (Fig. 3c). Overall, the pellets exhibited greater values compared to the filaments and LDPE exhibited greater  $I_{CO}$  values compared to all the types of HDPE MPs. Vinyl index for all HDPE and LDPE increased with exposure time. Comparingly, LDPE MPs had the highest vinyl index of 1.1. It is reported that photodegradation rate decreases with increasing the molecular orientation and crystalline fraction due to slow radical mobility (Garton et al., 1977). UV exposure increased photodegradation of both HDPE and LDPE but the rate of degradation was significant in LDPE compared to HDPE. The presence of labile H atoms in tertiary carbons of branched LDPE compared to linear HDPE renders the photooxidation reactions by improving the formation of carbonyl and vinyl groups. Besides that chain segment movement and radical mobility make LDPE more prone to photodegrade than HDPE (Rapoport et al., 1975). MPs photoinduced aging increased the cleavage of C–H bonds and this enhanced the formation of free radicals (Liu et al., 2019). Also, it is reported that the surface oxidation is a profound factor of aging MPs under ambient atmosphere in the presence of natural sunlight (Rjeb et al., 2000). Also, the filaments extruded at fast velocity have more ordered conformation

and a high degree of crystallinity which reduce the photodegradation rate compared to its pellet form. The formation of hydroxyl groups was not prominent on primary HDPE or LDPE surfaces. This may be due to the insufficient UV exposure duration for the development of the hydroxyl groups. The results from DSC analysis exhibited that LDPE pellets had the lowest crystallinity compared to their filament forms and all types of HDPE after UV exposure. This confirms that the pellets are less photostable compared to the filament form in both HDPE and LDPE.

**(B) XPS Analysis:** XPS analysis was conducted on both types of HDPE and LDPE forms to quantitatively study the surface atomic ratios, functional groups, and oxidation states of PE before and after photodegradation. Low-resolution survey scan (LR-XPS) of HDPE (Fig. S5, S6) and LDPE (Fig. S7, S8) pellets, filaments extruded with slow and fast velocities detect two distinct peaks for the presence of C 1s and O 1s at 284.7 and 531.2 eV, respectively. The presence of O 1s peak before photodegradation is due to intrinsic surface oxidation and the effect from the stabilizers, fillers, and impurities introduced during the PE manufacturing process to make it strong, more durable, and thermally resistant. Similar observations were reported for LDPE films and the influence of these additives on PE was not examined in the present study due to the limited project duration and resources (Salehi et al., 2018). High-resolution XPS of C 1s spectra were deconvoluted into four peaks to analyze the individual contribution of each functional group and to

calculate the abundance of each functionality upon surface oxidation. The C 1s peaks were deconvoluted with binding energies centered at 284.7 eV (C–C), 286.4 eV (C–O), 287.7 eV (C=O), and 289.2 eV (O–C=O), respectively, and the peak assignment matched well with previously reported literature (Azimi and Asselin, 2021; Hong and Hwang, 2021). The XPS peaks for oxygen were broadened and difficult to deconvolute and resolve by HR-XPS. Carbon and oxygen atomic percentages of MPs before and after photodegradation were estimated by LR survey scan. The atomic percentages of (C–O), (C=O), and (O–C=O) functionalities have increased for all forms of HDPE and LDPE after irradiating the samples with UV radiation due to surface oxidation (Table S5). The total carbon percentages decreased for all the samples after UV irradiation except for the HDPE filaments extruded at a fast velocity. This is due to the reaction of atmospheric oxygen with the radical species generated within the MPs (Ding et al., 2022b). Additionally, the oxygen percentages were increased accordingly due to the formation of oxygen containing functional groups (Hurley and Leggett, 2009). The polarity index of (O/C) of HDPE and LDPE pellets calculated from LR-XPS data were as 0.11, 0.16 before UV exposure and the ratios increased as 0.17, 0.24 after UV photodegradation which confirms that surface oxidation was high in LDPE compared to HDPE since abstraction of hydrogen from a tertiary carbon is more susceptible in LDPE. Additionally, this suggests that the surfaces of HDPE and LDPE have changed from less hydrophilic to more hydrophilic. The (O/C) ratio of HDPE and LDPE filaments with slow and fast post drawing velocities were changed from (0.15, 0.42) to (0.35, 0.26) for HDPE and from (0.19, 0.16) to (0.45, 0.47) for LDPE, respectively. The polarity index obtained for the filaments was high in both HDPE and LDPE compared to the pellets and it was significant in LDPE due to the recombination of radicals after photodegradation through decarbonylation or decarboxylation. According to the DSC analysis, it was revealed that the pellets are less photostable and have low crystallinity than the filaments. The low polarity index of pellets might be due to the formation of volatile photo-products in the form of CO<sub>2</sub> and CO after UV exposure (Grossetête et al., 2000). This can be dominant in less photostable pellets compared to the filaments. The results also support the above confirmation for increasing the surface oxidation except for the HDPE filament extruded at a fast velocity. All types of LDPE exhibited the highest increase in surface oxygen functionals compared to HDPE and this indicates that HDPE is

more photostable than LDPE. It should be noted that the XPS analysis was conducted only for one plastic sample in which analysis area was around 400 μm<sup>2</sup> with a maximum analytical penetration depth of 100 Å. Thus, it might involve some limitations due to the non-uniform photodegradation of plastic. For instance, the O/C ratio before and after photodegradation for HDPE filaments-fast were 0.42 and 0.25, respectively, however the carbonyl and vinyl indices for the fast extruded HDPE filaments were increased from 0.37 to 0.34 to 0.79 and 0.65 after 5 weeks of photodegradation. For the other MPs, the XPS analysis confirmed the ATR-FTIR results.

### 3.1.3. Surface morphology variation of PMPs due to the photodegradation

The surface morphology of primary HDPE and LDPE was analyzed using FE-SEM imaging (Fig. 4). Before photodegradation, both HDPE and LDPE surfaces were homogenous with little surface roughness and irregularities which are similar to MPs surfaces observed by other reporters (Ding et al., 2022a). Fig. S2 demonstrates the macromolecular morphology of HDPE and LDPE in the form of pellets and filaments before and after photodegradation. Since photodegradation proceeds from the surface to the core, crack formation is a surface phenomenon (Fujiwara and Zeronian, 1982). Chemicrystallization made densification of the MP surface layers and ultimately cracks were formed. Also, it is reported that they are formed spontaneously when exposed to UV irradiation due to an increase in the crystallinity (Fechine and Demarquette, 2008; Rabello and White, 1997b). This is further supported by the visual observation of more cracks perpendicular to the filament axis upon photodegradation in filaments extruded fast compared to those slow extruded HDPE and LDPE PMPs Fig. S2. As seen by SEM morphologies exposure to a moderate temperature at 50 °C and UV radiation for a prolonged period make contraction of the polymer surface layers and micro cracks are formed. (Schoolenberg and Meijer, 1991). The average diameter of the cracks formed for HDPE and LDPE pellets were obtained as 17.2 and 12.4 nm using ImageJ software. This further supports that the crack diameter obtained for HDPE was greater due to high crystallinity than LDPE after photodegradation.

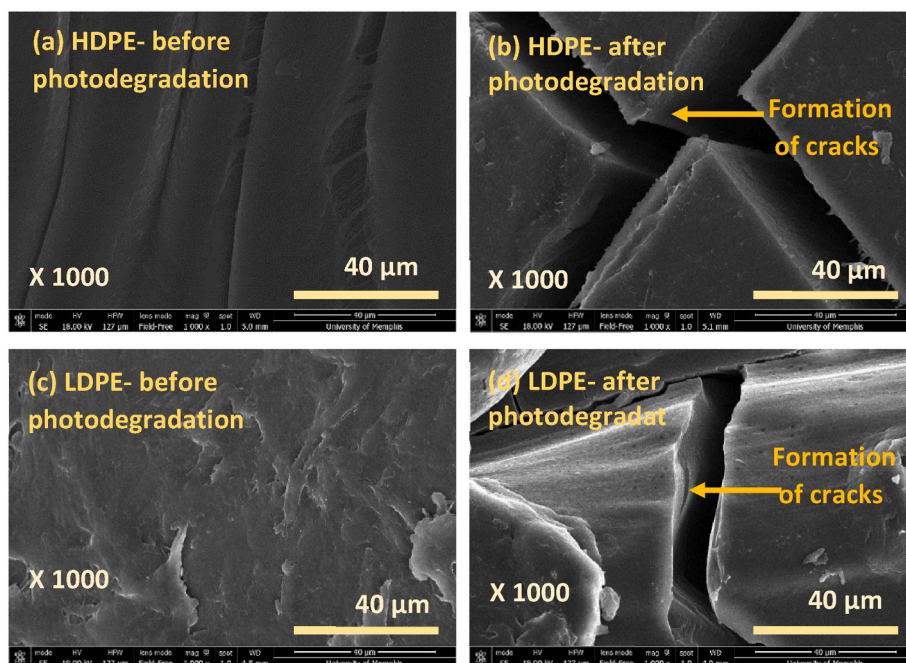


Fig. 4. FE-SEM micrographs of (a), (b) HDPE pellets, and (c), (d) LDPE pellets before and after UV photodegradation.

### 3.2. Extrinsic factors influence the photodegradation of MPs

#### 3.2.1. Characterization of SMPs

Secondary HDPE and LDPE pellets that were created by abrading through sand exhibited an intense band around  $1050\text{ cm}^{-1}$  for Si–O–Si stretching vibrations (Fig. 2b). This may be due to the remaining sand particle accumulation on MP surfaces even after rinsing with water. Additionally, a broad band appears in the region of  $3100\text{--}3650\text{ cm}^{-1}$  for –OH functions, and the presence of this band is due to the Si–OH groups introduced to MPs in the mechanical degradation process. The % crystallinity values obtained for both S-HDPE and S-LDPE were less than the PMPs (Fig. S9). This suggests that secondary MPs were less resistant to photodegradation compared to PMPs.

Fig. S10 represents the SEM images of secondary HDPE and LDPE with nonhomogeneous rough surfaces. The main difference between these images from the primary PE is the presence of agglomerated sand particles after mechanical degradation occurred due to the abrasion of PE with sand. Additionally, the abrasion with silty sand for a long period creates micropores, grooves, and surface deformation with rough heterogeneous surfaces where the smaller silt particles can deposit and settle on MPs surfaces (Aghilinasrollahabadi et al., 2021). This sand accumulation persisted even after rinsing with water and ultrasound sonication treatment and was not completely removed. Also, this was further supported by the visual discoloration to orange/brown from initial white for both HDPE and LDPE as seen in Fig. S2. After photodegradation, noticeable alterations were observed for both types of PE including more cracks and wrinkles on the surface. Under the influence of external pressure and heat, the characteristics structure, and reactivity of plastics can be changed, and they can be degraded into smaller sizes.

Secondary PE pellets of HDPE and LDPE generated by abrading with sand were subjected to photodegradation for five weeks. Change in % crystallinity of both HDPE and LDPE is tabulated in Table S3, S4. As with primary PE, the crystallinity increased when accelerating the photodegradation. It is reported that the polar groups introduced in SMPs can interact with dipolar forces and undergo further crystallization (Gulmine et al., 2003). The formation of oxidation products increases the crystal defects in the polymer by generating small crystals with more imperfections. This leads to low melting temperatures of the polymer after photodegradation (Fig. S11) (Ojeda et al., 2011).

#### 3.2.2. Surface chemistry variation of SMPs due to the photodegradation

After irradiating the HDPE and LDPE SMPs, a new band appeared in the region of  $1600\text{--}1750\text{ cm}^{-1}$  for acids/esters/ketones demonstrating

the formation of new functionalities as a result of photodegradation (Aghilinasrollahabadi et al., 2021; Grigoriadou et al., 2018). The nature of the external substrates or objects attached to the surfaces influences the optical properties of that compound. Photodegradation of pyrene in the presence of oxygen has increased when coated with  $\text{Al}_2\text{O}_3$  or  $\text{SiO}_2$  due to the enhanced formation of hydroxyl radicals (Romanias et al., 2014). Additionally, high photodegradation of PFOA on quartz sand particles was observed due to high light transmittance but this was not the only factor that determined the efficiency of photochemical decompositions (Liu et al., 2020b). Nevertheless, the organic carbon (OC) has an inhibitory effect on MPs photodegradation since OC makes chelation and H bond interactions with MPs which shields and make chemical bond related stabilization and suppress UV photodegradation (Ding et al., 2022a). In secondary HDPE and LDPE, carbonyl index calculated at  $1712\text{ cm}^{-1}$  increased with time and likewise, S-LDPE exhibited the highest  $I_{\text{CO}}$  (Fig. 5). When comparing the results of carbonyl indices obtained for both primary and secondary HDPE and LDPE pellets after 5 weeks of photodegradation, SPE exhibited slightly high values compared to the PPE and this is due to the attachment of silty sand particles on MPs surfaces which enhanced UV absorbance. In the ATR-FTIR spectrum, a sharp band was not observed in the carbonyl region for S-HDPE and S-LDPE, and this may be due to the formation of multiple unsaturated groups upon photodegradation. The vinyl index for SPE was not quantitatively analyzed since the peak was overlapped with Si–O–Si stretching vibrations in that region. The hydroxyl index gradually increased for S-HDPE and but for S-LDPE it dropped after the first week of UV exposure and then slightly increased after three weeks and this may be due to the utilization of hydroxyl groups as hydroxyl/peroxyl radicals for the destruction of the carbon backbone.

### 3.3. MPs photodegradation mechanism

MP degradation is highly confined to amorphous regions and can be divided into three stages initiation, propagation, and termination (Pritchard, 2012). Additionally, the rate of degradation is influenced by the external objects attached to MPs surfaces as they can alter the degradation by improving the formation of reactive oxygen species that are responsible for photodegradation. Polyethylene MPs are composed of  $-\text{CH}_2$  monomers oriented in the C–C backbone and unsaturated double bonds, or chromophores are not present in the polymer to absorb the UV radiation, hence it is resistant to photodegradation. Nevertheless, the presence of low-level impurities, structural defects incorporated in the manufacturing process act as chromophores to initiate photodegradation to some extent (Fairbrother et al., 2019). Upon exposure to

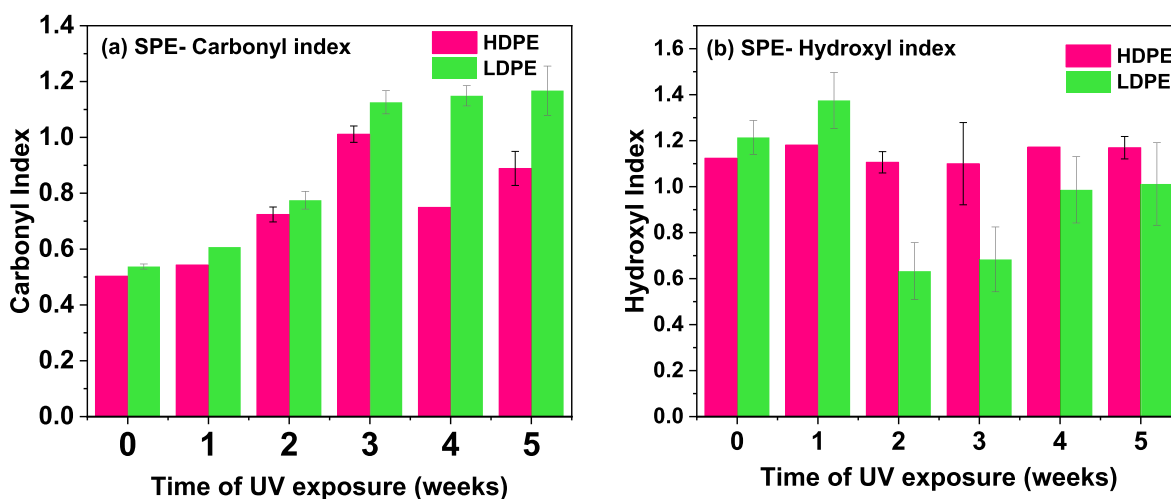


Fig. 5. (a) Carbonyl and (b) hydroxyl indices for secondary MPs produced as pellets for HDPE and LDPE after exposure to UV degradation. Error bars are from standard deviation from three replicates.

UV irradiation, chemical bonds in the polymer absorb UV energy and polymer free radicals are generated in the initiation step (Singh and Sharma, 2008). In the propagation step, peroxy radicals are formed due to the reaction of polymer radicals and oxygen. This leads to chain scission and will decrease the molecular weight of the polymer (Tolinski, 2015). Two radicals can combine to form oxygenated low molecular weight products such as ketones, olefins, aliphatic carboxylic acids, alcohols, and aldehydes in the termination step (Gewert et al., 2015). These functional groups are more susceptible to photodegradation due to the presence of chromophores and unsaturated double bonds. The bond energy of C–C and C–H functionals in PE is around 300 kJ/mol which requires high energy to decompose them and UV B radiation at a wavelength of 285 nm is equivalent for the bond destruction. UV A radiation is not sufficient in terms of energy and UV C radiation with high energy is not used in this study as it limits to simulate practical conditions in real-world applications since most of it is filtered in the upper atmosphere and doesn't reach the ground level. Also, it is reported that the surface oxidation is a profound factor of aging MPs under ambient atmosphere in the presence of natural sunlight (Rjeb et al., 2000). Thermo oxidative reactions of plastics will take place if the thermal energy is sufficient to overcome the energy barrier of polymers. At elevated temperatures, polymer chains break apart to give free radicals and in the presence of oxygen, they can form hydroperoxide (Pirsaheb et al., 2020). This thermal degradation of plastic materials also generate hydroxyl and alkoxy radicals similarly to photodegradation which leads to fragmentation and generates polymer free radicals and the reactions self propagate until inert products are formed by the combination of two radicals and as a result of chain scission and cross linking, polymer molecular weight reduces and crystallinity increases (Crawford and Quinn, 2016; Zhang et al., 2021).

### 3.4. Investigation of heavy metal uptake by MPs

Heavy metal adsorption on MPs aged by UV radiation depends under different environmental conditions such as air, pure water, and sea water (Mao et al., 2020). It is reported that higher amounts of Cu(II), and Zn(II) accumulation occurred on UV aged PET debris than virgin PET due to presence of oxygen-containing groups (Wang et al., 2020). Also, Pb(II) adsorption has increased on UV aged PE due to the increase in MPs surface area and hydrophilicity (Guan et al., 2022). PS aged under H<sub>2</sub>O<sub>2</sub> followed by UV oxidation demonstrated increase in surface functionalities rather than surface area for the sorption of organic contaminants (Hüffer et al., 2018). Adsorption of pharmaceuticals occurred on MPs aged by photo-Fenton reaction and UVA radiation through electrostatic interactions and H bonding (Fan et al., 2021; Liu et al., 2020c).

Heavy metal uptake by HDPE and LDPE before and after photodegradation was monitored at different time intervals. Fig. 6 demonstrates the metal loading capacities of MPs in synthetic stormwater at pH 7. The composition of synthetic stormwater is present in supporting information (Table S6). New LDPE pellets (PMPs) exhibited high Pb(II) uptake when increasing the duration to metal exposure due to surface physisorption and no Zn(II) adsorption occurred throughout the five-day exposure period. The metal uptake capacities for new HDPE pellets were lower than the limits of detection (LOD) for both Pb(II)-3.1 µg/L and Zn(II)- 9.6 µg/L. Nevertheless, UV photodegradation enhanced Pb(II), Zn(II) uptake for LDPE pellets, and Pb(II) uptake for HDPE pellets. UV photodegradation of MPs generated surface oxygen functionalities which enhanced the polarity, surface charge, and hydrophilicity thus making the MPs more susceptible for metal uptake via electrostatic attractions and surface complexation (Li et al., 2018). But the ion competition resulted in an insignificant amount of Zn(II) adsorption onto HDPE and this observation was reported in previous literature when both Pb(II) and Zn(II) were present in a mixture (Aghilinasrollahabadi et al., 2021; Ahamed et al., 2020; Zhou et al., 2020). Nevertheless, it is reported that the Cu(II) adsorption on MPs has significantly reduced in the presence of competitive Ca(II) and Mg(II) (Yang et al., 2019). Photodegraded LDPE pellets exhibited high Pb(II) and Zn(II) surface loadings as they contain more surface functional groups upon oxidation compared to HDPE.

As we suggested in our previous publications, the adsorption of the heavy metals onto the surface of the new plastic is controlled via physical confinement and weak van der Waals interactions (Hadiuzzaman et al., 2022; Aghilinasrollahabadi et al., 2021). Thus, the plastic with a less crystalline structure, larger volume of surface cavities, and more surface roughness allows greater adsorption of heavy metals. Furthermore, the generation of oxidized surface functional groups onto the plastic surface during the production process or accelerated aging process could promote the adsorption of the heavy metals by increasing the electrostatic interactions and physical confinement caused by increasing the surface roughness (Hadiuzzaman et al., 2022; Ainali et al., 2021). Besides the functionalities introduced by photodegradation, the high initial crystallinity of HDPE compared to LDPE limits mass transfer of heavy metal ions from the bulk solution into the MPs surfaces and this resulted in very low metal uptake onto the surface. The greater crystallinity of HDPE reduced the available free volume and limited the adsorption process. However, the greater free volume available within the LDPE structure promoted the heavy metals adsorption process. A study conducted on different types of MPs on Cd(II) adsorption reported that metal uptake capacity reduced when increasing the crystallinity in the order of PVC < PS < PP < PE (Guo

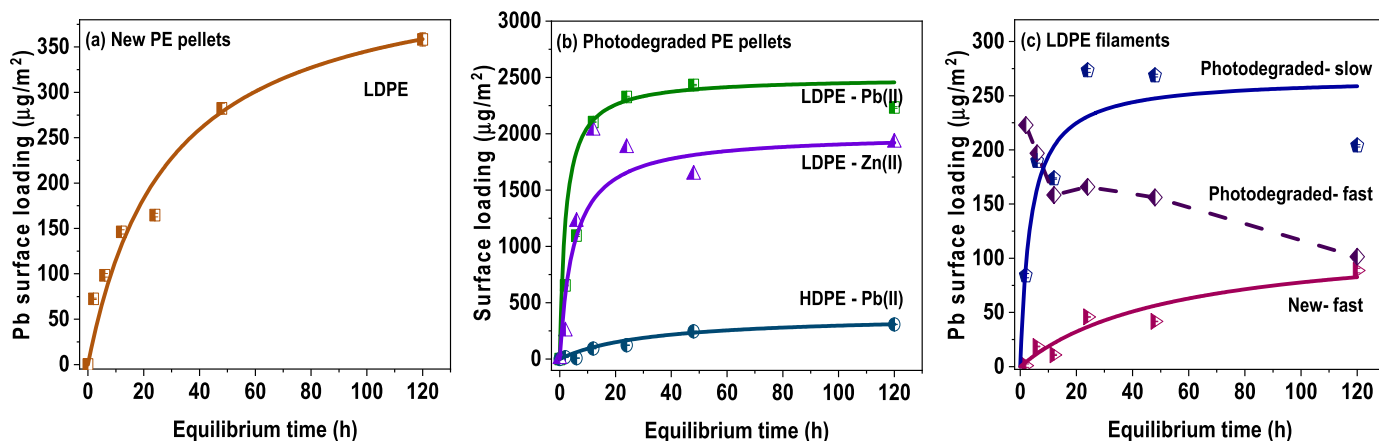


Fig. 6. Surface loading of heavy metal on PE (a) New LDPE pellets, (b) After photodegradation of LDPE and HDPE pellets, and (c) New and photodegraded LDPE filaments extruded with different chain orientation. 300 µg/L of Pb(II) or Zn(II) solution (12 mL) at pH 7 was mixed at a stirring rate of 200 rpm with MPs pellets or filaments (300 mg) at different time intervals. Error bars are the standard deviation of three replicates.

et al., 2020). Hence, LDPE was selected to further investigate the behavior of different forms of MPs on metal adsorption.

LDPE filaments extruded under slow and fast velocities before and after photodegradation were subjected to five-day metal exposure experiments. The new filaments except LDPE extruded at fast velocity exhibited no metal uptake as they were below the limit of detections of both Pb(II) and Zn(II). This may be due to the high crystallinity of new filaments compared to the pellet form as analyzed by the DSC. The percent crystallinity (%23.4) and carbonyl index (0.33) of the fast extruded LDPE filaments were slightly greater than those extruded slowly (%20.5, CI = 0.29). Despite the increased crystallinity of fast extruded filaments, their greater surface oxidation and roughness compared to the slow extruded filament may have contributed in their elevated Pb uptake. The FE-SEM images of new and photodegraded filaments are shown in **Figure SI-11**. After photodegradation, the slow extruded LDPE filaments exhibited high Pb(II) adsorption capacity with 273.5  $\mu\text{g}/\text{m}^2$  of surface loading due to the surface functionalities. The photodegraded LDPE filaments generated at fast velocity exhibited high Pb(II) adsorption with 222  $\mu\text{g}/\text{m}^2$  during the first 2 h and it gradually decreased up to 101  $\mu\text{g}/\text{m}^2$  through the exposure of 120 h. This was due to the release of Pb(II) during longer exposure durations. The photodegraded LDPE pellets exhibited the highest metal uptake compared to the filaments generated for both Pb(II) and Zn(II) with surface loadings of 2526 and 2028  $\mu\text{g}/\text{m}^2$  respectively, at equilibrium. Rather than increased electrostatic interaction with heavy metals present within the aqueous solution due to the MPs' photodegradation, studying the surface morphology of photodegraded MPs suggested a greater physical confinement of heavy metal ions due to the increased roughness and surface area caused by surface cracking and deformation. It should be noted that, although 300 mg of all MPs were added to the metal aqueous solution, the smaller diameter of fast extruded filaments provided a greater surface area to volume ratio for those compared to the pellets and slow extruded filaments, thus the results have been present as metal loading per unit area and not mass to consider the effect of different surface area of different forms of plastic. The surface area in this study has been estimated for the pellets and filament segments as spheres, and cylinders as accurate quantifications of surface area was not possible due to the lack of resources. Thus, it involves a limitation for not considering the changes in surface area due to the photodegradation process. However, the results demonstrating the heavy metals adsorption kinetics onto the plastic samples reported as  $\mu\text{g}/\text{mg}$  are shown in **Figure SI-13**.

Pseudo first and second-order kinetic models were applied to describe the metal uptake mechanism to the MPs. All types of MPs fitted well to pseudo second-order kinetic model,  $t/q_t = t/q_e + 1/k_2q_e^2$  with high linear regression coefficients of  $R^2 > 0.90$ . Here,  $t$  is the contact time (h),  $q_e$  denotes the surface loading ( $\mu\text{g}/\text{m}^2$ ) at the equilibrium time,  $q_t$  is the amount adsorbed at time  $t$  ( $\mu\text{g}/\text{m}^2$ ) and  $k_2$  is the second-order rate constant ( $\text{m}^2/\mu\text{g h}$ ). This indicates the rate-limiting step for metal uptake is predominantly through chemisorption with the active sites present on MPs surface via electrostatic interactions, metal complexation, or chelation (Cao et al., 2021; Liu et al., 2022). The data and parameters obtained for kinetic studies are tabulated in **Table S6**. This study demonstrated the plastics' microstructure as dominant factor that controls the extent of heavy metals adsorption onto the new plastics, in which the LDPE MPs with a branched and less crystalline structure adsorbed a greater level of Pb than HDPE MPs with a linear structure and more crystallinity. Although, creation of oxidized surface functional groups onto the MPs due to the photodegradation promoted their heavy metals uptake, still the plastic microstructure played the dominant role as heavy metals adsorption onto the photodegraded LDPE MPs exceeded the photodegraded HDPE MPs.

#### 4. Conclusion

The environmental stability of plastics is directly linked to their structural properties and the forces they are exposed to while they remain in the environment. Thus, this study elucidated the role of intrinsic and extrinsic factors that influence the kinetics of PMPs and SMPs photodegradation using advanced surface analysis techniques. Enhanced crystallinity was observed for MPs by increasing the duration of UV exposure, while photodegradation rate decreased with increasing the orientation and crystalline fraction in the amorphous content. In contrast to the pellet form for HDPE and LDPE, filaments extruded at slow and fast post drawing velocities exhibited high initial crystallinity and it gradually increased upon exposure to UV as molecular orientation increased due to chain scission followed by chemocrystallization. Additionally, MPs photodegradation increased by sediment attachment as this enhanced the formation of reactive oxygen species. A greater degree of branching and less crystalline fraction in LDPE made it less photostable compared to the linear structure of HDPE. This made LDPE pellets high susceptible for heavy metal uptake in stormwater with a surface loading of 2526 and 2028  $\mu\text{g}/\text{m}^2$  for Pb(II) and Zn(II) respectively. While having the plastics that are degrading faster is beneficial as it limits the long-term environmental impacts, it should be considered that degraded plastics are transporting a greater level of contaminant from urban environment to the adjacent water resources. The knowledge developed in this study by better understanding the link between the plastic's original characteristics, physiochemistry variations during use and disposal within the environment, and susceptibility to the heavy metals adsorption from stormwater could be utilized to inform the manufacturers to design the plastic products for less environmental impacts while maintaining the required performance characteristics.

#### Author statement

**Amali Hearth:** Methodology, Investigation, Writing original draft, Visualization **Maryam Salehi:** Conceptualization, Methodology, Resources, Review and Editing, Supervision

#### Declaration of competing interest

The authors declare that they have no known competing financial interests or personal relationships that could have appeared to influence the work reported in this paper.

#### Acknowledgment

The authors would like to thank Dr. Felio Perez, Dr. Omar Skalli for assistance with FESEM and XPS analysis. The authors also thank Dr. Tomoko Fujiwara for providing access to DSC instrument. Funding for this work was provided by the National Science Foundation grant CBET-2044836 and the United States Department of Agriculture, National Institute of Food and Agriculture, USDA/NIFA) Award number 2020-67019-31166.

#### Appendix A. Supplementary data

Supplementary data to this article can be found online at <https://doi.org/10.1016/j.envpol.2022.119628>.

#### References

- Abbasi Mahmoodabadi, H., Haghghat Kish, M., Aslanzadeh, S., 2018. Photodegradation of partially oriented and drawn polypropylene filaments. *J. Appl. Polym. Sci.* 135, 45716.
- Aghilinasrollahabadi, K., Salehi, M., Fujiwara, T., 2021. Investigate the influence of microplastics weathering on their heavy metals uptake in stormwater. *J. Hazard Mater.* 408, 124439.

- Ahamed, T., Brown, S.P., Salehi, M., 2020. Investigate the role of biofilm and water chemistry on lead deposition onto and release from polyethylene: an implication for potable water pipes. *J. Hazard Mater.* 400, 123253.
- Ainali, N.M., Bikiaris, D.N., Lambropoulou, D.A., 2021. Aging effects on low-and high-density polyethylene, polypropylene and polystyrene under UV irradiation: an insight into decomposition mechanism by Py-GC/MS for microplastic analysis. *J. Anal. Appl. Pyrol.*, 105207
- Azimi, M., Asselin, E., 2021. Chemical oxidation of high-density polyethylene: surface energy, functionality, and adhesion to liquid epoxy. *J. Appl. Polym. Sci.*, 50999
- Babaghayou, M.I., Mourad, A.-H.I., Lorenzo, V., de la Orden, M.U., Urreaga, J.M., Chabira, S.F., Sebaa, M., 2016. Photodegradation characterization and heterogeneity evaluation of the exposed and unexposed faces of stabilized and unstabilized LDPE films. *Mater. Des.* 111, 279–290.
- Barbieri, Y., Massad, W.A., Díaz, D.J., Sanz, J., Amat-Guerri, F., García, N.A., 2008. Photodegradation of bisphenol A and related compounds under natural-like conditions in the presence of riboflavin: kinetics, mechanism and photoproducts. *Chemosphere* 73, 564–571.
- Benítez, A., Sánchez, J.J., Arnal, M.L., Müller, A.J., Rodríguez, O., Morales, G., 2013. Abiotic degradation of LDPE and LLDPE formulated with a pro-oxidant additive. *Polym. Degrad. Stabil.* 98, 490–501.
- Bonyadinejad, G., Salehi, M., Herath, A., 2022. Investigating the sustainability of agricultural plastic products, combined influence of polymer characteristics and environmental conditions on microplastics aging. *Sci. Total Environ.* 839, 156385.
- Cao, Y., Zhao, M., Ma, X., Song, Y., Zuo, S., Li, H., Deng, W., 2021. A Critical Review on the Interactions of Microplastics with Heavy Metals: Mechanism and Their Combined Effect on Organisms and Humans. *Science of The Total Environment*, 147620.
- Carrasco, F., Pages, P., Pascual, S., Colom, X., 2001. Artificial aging of high-density polyethylene by ultraviolet irradiation. *Eur. Polym. J.* 37, 1457–1464.
- Chiellini, E., Corti, A., D'Antone, S., Baciur, R., 2006. Oxo-biodegradable carbon backbone polymers—Oxidative degradation of polyethylene under accelerated test conditions. *Polym. Degrad. Stabil.* 91, 2739–2747.
- Crawford, C.B., Quinn, B., 2016. *Microplastic Pollutants*. Elsevier Limited.
- D'Amelia, R.P., Gentile, S., Nirode, W.F., Huang, L., 2016. Quantitative analysis of copolymers and blends of polyvinyl acetate (PVAc) using Fourier transform infrared spectroscopy (FTIR) and elemental analysis (EA). *World J. Chem. Educ.* 4, 25–31.
- Devriese, L.L., De Witte, B., Vethaak, A.D., Hostens, K., Leslie, H.A., 2017. Bioaccumulation of PCBs from microplastics in Norway lobster (*Nephrops norvegicus*): an experimental study. *Chemosphere* 186, 10–16.
- Ding, L., Ouyang, Z., Liu, P., Wang, T., Jia, H., Guo, X., 2022a. Photodegradation of microplastics mediated by different types of soil: the effect of soil components. *Sci. Total Environ.* 802, 149840.
- Ding, L., Yu, X., Guo, X., Zhang, Y., Ouyang, Z., Liu, P., Zhang, C., Wang, T., Jia, H., Zhu, L., 2022b. The photodegradation processes and mechanisms of polyvinyl chloride and polyethylene terephthalate microplastic in aquatic environments: important role of clay minerals. *Water Res.* 208, 117879.
- Duan, J., Li, Y., Gao, J., Cao, R., Shang, E., Zhang, W., 2022. ROS-mediated photoaging pathways of nano-and micro-plastic particles under UV irradiation. *Water Res.* 216, 118320.
- Eerkes-Medrano, D., Thompson, R.C., Aldridge, D.C., 2015. Microplastics in freshwater systems: a review of the emerging threats, identification of knowledge gaps and prioritisation of research needs. *Water Res.* 75, 63–82.
- Fairbrother, A., Hsueh, H.-C., Kim, J.H., Jacobs, D., Perry, L., Goodwin, D., White, C., Watson, S., Sung, L.-P., 2019. Temperature and light intensity effects on photodegradation of high-density polyethylene. *Polym. Degrad. Stabil.* 165, 153–160.
- Fan, X., Zou, Y., Geng, N., Liu, J., Hou, J., Li, D., Yang, C., Li, Y., 2021. Investigation on the adsorption and desorption behaviors of antibiotics by degradable MPs with or without UV ageing process. *J. Hazard Mater.* 401, 123363.
- Fechine, G., Demarquette, N., 2008. Cracking formation on the surface of extruded photodegraded polypropylene plates. *Polym. Eng. Sci.* 48, 365–372.
- Fujiwara, Y., Zeronian, S., 1982. Formation of cracks on photodegraded nylon 6 filaments. *J. Appl. Polym. Sci.* 27, 2773–2782.
- Gallo, F., Fossi, C., Weber, R., Santillo, D., Sousa, J., Ingram, I., Nadal, A., Romano, D., 2018. Marine litter plastics and microplastics and their toxic chemicals components: the need for urgent preventive measures. *Environ. Sci. Eur.* 30, 1–14.
- Garton, A., Carlsson, D., Sturgeon, P., Wiles, D., 1977. The photo-oxidation of polypropylene monofilaments: Part III: effects of filament morphology. *Textil. Res. J.* 47, 423–428.
- Gewert, B., Plassmann, M.M., MacLeod, M., 2015. Pathways for degradation of plastic polymers floating in the marine environment. *Environmental science: Process. Impacts* 17, 1513–1521.
- Gidigbi, J.A., Martins, A., Enyoh, C.E., 2020. A problem in disguise: a review paper on generous uses of polyethylene bags (nylon bags) in Nigeria and its environmental implications. *AIMS Environmental Science* 7, 602–610.
- Gong, J., Xie, P., 2020. Research progress in sources, analytical methods, eco-environmental effects, and control measures of microplastics. *Chemosphere* 254, 126790.
- Grigoriadou, I., Pavlidou, E., Paraskevopoulos, K.M., Terzopoulou, Z., Bikiaris, D.N., 2018. Comparative study of the photochemical stability of HDPE/Ag composites. *Polym. Degrad. Stabil.* 153, 23–36.
- Grossetête, T., Rivaton, A., Gardette, J., Hoyle, C.E., Ziemer, M., Fagerburg, D., Clauberg, H., 2000. Photochemical degradation of poly (ethylene terephthalate)-modified copolymer. *Polymer* 41, 3541–3554.
- Guan, Y., Gong, J., Song, B., Li, J., Fang, S., Tang, S., Cao, W., Li, Y., Chen, Z., Ye, J., 2022. The effect of UV exposure on conventional and degradable microplastics adsorption for Pb (II) in sediment. *Chemosphere* 286, 131777.
- Gulmine, J., Janissek, P., Heise, H., Akcelrud, L., 2003. Degradation profile of polyethylene after artificial accelerated weathering. *Polym. Degrad. Stabil.* 79, 385–397.
- Guo, X., Hu, G., Fan, X., Jia, H., 2020. Sorption properties of cadmium on microplastics: the common practice experiment and a two-dimensional correlation spectroscopic study. *Ecotoxicol. Environ. Saf.* 190, 110118.
- Hadiuzzaman, Md, Salehi, Maryam, Fujiwara, Tomoko, 2022. Plastic litter fate and contaminant transport within the urban environment, photodegradation, fragmentation, and heavy metal uptake from storm runoff. *Environ. Res.* 212, 113183.
- Holmes, L.A., Turner, A., Thompson, R.C., 2012. Adsorption of trace metals to plastic resin pellets in the marine environment. *Environ. Pollut.* 160, 42–48.
- Hong, S.-H., Hwang, S.-H., 2021. Enhancing the mechanical performance of surface-modified microcrystalline cellulose reinforced high-density polyethylene composites. *Mater. Today Commun.* 27, 102426.
- Huang, D., Tao, J., Cheng, M., Deng, R., Chen, S., Yin, L., Li, R., 2020. Microplastics and nanoplastics in the environment: macroscopic transport and effects on creatures. *J. Hazard Mater.*, 124399
- Hüffer, T., Weniger, A.-K., Hofmann, T., 2018. Sorption of organic compounds by aged polystyrene microplastic particles. *Environ. Pollut.* 236, 218–225.
- Hurley, C.R., Leggett, G.J., 2009. Quantitative investigation of the photodegradation of polyethylene terephthalate film by friction force microscopy, contact-angle goniometry, and X-ray photoelectron spectroscopy. *ACS Appl. Mater. Interfaces* 1, 1688–1697.
- Kalčíková, G., Alič, B., Skalar, T., Bundschuh, M., Gotvajn, A.Ž., 2017. Wastewater treatment plant effluents as source of cosmetic polyethylene microbeads to freshwater. *Chemosphere* 188, 25–31.
- Li, J., Zhang, K., Zhang, H., 2018. Adsorption of antibiotics on microplastics. *Environ. Pollut.* 237, 460–467.
- Liu, G., Zhu, Z., Yang, Y., Sun, Y., Yu, F., Ma, J., 2019. Sorption behavior and mechanism of hydrophilic organic chemicals to virgin and aged microplastics in freshwater and seawater. *Environ. Pollut.* 246, 26–33.
- Liu, H., Liu, K., Fu, H., Ji, R., Qu, X., 2020a. Sunlight mediated cadmium release from colored microplastics containing cadmium pigment in aqueous phase. *Environ. Pollut.* 263, 114484.
- Liu, J., Xiang, W., Li, C., Van Hoomissen, D.J., Qi, Y., Wu, N., Al-Basher, G., Qu, R., Wang, Z., 2020b. Kinetics and mechanism analysis for the photodegradation of PFOA on different solid particles. *Chem. Eng. J.* 383, 123115.
- Liu, P., Lu, K., Li, J., Wu, X., Qian, L., Wang, M., Gao, S., 2020c. Effect of aging on adsorption behavior of polystyrene microplastics for pharmaceuticals: adsorption mechanism and role of aging intermediates. *J. Hazard Mater.* 384, 121193.
- Liu, P., Shi, Y., Wu, X., Wang, H., Huang, H., Guo, X., Gao, S., 2021. Review of the Artificially-Accelerated Aging Technology and Ecological Risk of Microplastics. *Science of the Total Environment*, 144969.
- Liu, S., Huang, J., Zhang, W., Shi, L., Yi, K., Yu, H., Zhang, C., Li, S., Li, J., 2022. Microplastics as a vehicle of heavy metals in aquatic environments: a review of adsorption factors, mechanisms, and biological effects. *J. Environ. Manag.* 302, 113995.
- Ma, Y., Huang, A., Cao, S., Sun, F., Wang, L., Guo, H., Ji, R., 2016. Effects of nanoplastics and microplastics on toxicity, bioaccumulation, and environmental fate of phenanthrene in fresh water. *Environ. Pollut.* 219, 166–173.
- Madras, G., Chung, G., Smith, J., McCoy, B.J., 1997. Molecular weight effect on the dynamics of polystyrene degradation. *Ind. Eng. Chem. Res.* 36, 2019–2024.
- Mao, R., Lang, M., Yu, X., Wu, R., Yang, X., Guo, X., 2020. Aging mechanism of microplastics with UV irradiation and its effects on the adsorption of heavy metals. *J. Hazard Mater.* 393, 122515.
- Martínez-Romo, A., González-Mota, R., Soto-Bernal, J.J., Rosales-Candelas, I., 2015. Investigating the degradability of HDPE, LDPE, PE-BIO, and PE-OXO films under UV-B radiation. *Journal of Spectroscopy* 2015, 586514.
- Martínez, K., González, R., Soto, J., Rosales, I., 2021. Characterization by FTIR spectroscopy of degradation of polyethylene films exposed to CO2 laser radiation and domestic composting. *J. Phys. Conf.* 012038. IOP Publishing.
- Mateker, W.R., Heumueller, T., Cheacharoen, R., Sachs-Quintana, I., McGehee, M.D., Warnan, J., Beaujuge, P.M., Liu, X., Bazan, G.C., 2015. Molecular packing and arrangement govern the photo-oxidative stability of organic photovoltaic materials. *Chem. Mater.* 27, 6345–6353.
- Meng, Y., Kelly, F.J., Wright, S.L., 2020. Advances and challenges of microplastic pollution in freshwater ecosystems: a UK perspective. *Environ. Pollut.* 256, 113445.
- Min, K., Cuffi, J.D., Mathers, R.T., 2020. Ranking environmental degradation trends of plastic marine debris based on physical properties and molecular structure. *Nat. Commun.* 11, 1–11.
- Ojeda, T., Freitas, A., Birck, K., Dalmolin, E., Jacques, R., Bento, F., Camargo, F., 2011. Degradability of linear polyolefins under natural weathering. *Polym. Degrad. Stabil.* 96, 703–707.
- Panda, B.P., Mohanty, S., Nayak, S.K., 2014. Polyolefin nanocomposites with enhanced photostability weathering effect on morphology and mechanical properties. *J. Mater. Eng. Perform.* 23, 3229–3244.
- Pirsaheb, M., Hossini, H., Makhdoumi, P., 2020. Review of microplastic occurrence and toxicological effects in marine environment: experimental evidence of inflammation. *Process Saf. Environ. Protect.* 142, 1–14.
- Pritchard, G., 2012. *Plastics Additives: an AZ Reference*. Springer Science & Business Media.

- Rabello, M., White, J., 1997a. Crystallization and melting behaviour of photodegraded polypropylene—I. Chemi-crystallization. *Polymer* 38, 6379–6387.
- Rabello, M., White, J., 1997b. The role of physical structure and morphology in the photodegradation behaviour of polypropylene. *Polym. Degrad. Stabil.* 56, 55–73.
- Rajesh, C., 2019. Solid-phase photodegradation of polystyrene by nano TiO<sub>2</sub> under ultraviolet radiation. *Environ. Nanotechnol. Monit. Manag.* 12, 100229.
- Rapoport, N.Y., Berulava, S., Kovarskii, A., Musayelyan, I., Yershov, Y.A., Miller, V., 1975. The kinetics of thermo-oxidative degradation of oriented polypropylene in relation to the structure and molecular mobility of the polymer. *Polym. Sci.* 17, 2901–2909.
- Rjeb, A., Tajounte, L., El Idrissi, M.C., Letarte, S., Adnot, A., Roy, D., Claire, Y., Périchaud, A., Kaloustian, J., 2000. IR spectroscopy study of polypropylene natural aging. *J. Appl. Polym. Sci.* 77, 1742–1748.
- Romanias, M.N., Andrade-Eiroa, A.A., Shahla, R., Bedjanian, Y., Zogka, A.G., Philippidis, A., Dagaut, P., 2014. Photodegradation of pyrene on Al<sub>2</sub>O<sub>3</sub> surfaces: a detailed kinetic and product study. *J. Phys. Chem.* 118, 7007–7016.
- Rummel, C.D., Jahnke, A., Gorokhova, E., Kühnel, D., Schmitt-Jansen, M., 2017. Impacts of biofilm formation on the fate and potential effects of microplastic in the aquatic environment. *Environ. Sci. Technol. Lett.* 4, 258–267.
- Salehi, M., Jafvert, C.T., Howarter, J.A., Whelton, A.J., 2018. Investigation of the factors that influence lead accumulation onto polyethylene: implication for potable water plumbing pipes. *J. Hazard Mater.* 347, 242–251.
- Schoolenberg, G.E., Meijer, H.D.F., 1991. Ultra-violet degradation of polypropylene: 2. Residual strength and failure mode in relation to the degraded surface layer. *Polymer* 32, 438–444.
- Shimada, S., Hori, Y., Kashiwabara, H., 1988. Distribution of molecular orientation and stability of peroxy radicals in the noncrystalline region of elongated polypropylene. *Macromolecules* 21, 979–982.
- Singh, B., Sharma, N., 2008. Mechanistic implications of plastic degradation. *Polym. Degrad. Stabil.* 93, 561–584.
- Statista, 2021. Annual Production of Plastics Worldwide from 1950 to 2020 (in million metric tons).
- Sun, Y., Yuan, J., Zhou, T., Zhao, Y., Yu, F., Ma, J., 2020. Laboratory simulation of microplastics weathering and its adsorption behaviors in an aqueous environment: a systematic review. *Environ. Pollut.* 265, 114864.
- Suresh, B., Maruthamuthu, S., Khare, A., Palanisamy, N., Muralidharan, V., Ragunathan, R., Kannan, M., Pandiyaraj, K.N., 2011. Influence of thermal oxidation on surface and thermo-mechanical properties of polyethylene. *J. Polym. Res.* 18, 2175–2184.
- Tolinski, M., 2015. Additives for Polyolefins: Getting the Most Out of Polypropylene, Polyethylene and TPO. William Andrew.
- Turner, A., Holmes, L.A., 2015. Adsorption of trace metals by microplastic pellets in fresh water. *Environ. Chem.* 12, 600–610.
- Wang, J., Wang, M., Ru, S., Liu, X., 2019. High levels of microplastic pollution in the sediments and benthic organisms of the South Yellow Sea, China. *Sci. Total Environ.* 651, 1661–1669.
- Wang, Q., Zhang, Y., Wangjin, X., Wang, Y., Meng, G., Chen, Y., 2020. The adsorption behavior of metals in aqueous solution by microplastics effected by UV radiation. *J. Environ. Sci.* 87, 272–280.
- Webb, H.K., Arnott, J., Crawford, R.J., Ivanova, E.P., 2013. Plastic degradation and its environmental implications with special reference to poly (ethylene terephthalate). *Polymers* 5, 1–18.
- Yang, J., Cang, L., Sun, Q., Dong, G., Ata-Ul-Karim, S.T., Zhou, D., 2019. Effects of soil environmental factors and UV aging on Cu<sup>2+</sup> adsorption on microplastics. *Environ. Sci. Pollut. Control Ser.* 26, 23027–23036.
- Yousif, E., Haddad, R., 2013. Photodegradation and photostabilization of polymers, especially polystyrene. SpringerPlus 2, 1–32.
- Zhang, K., Hamidian, A.H., Tubić, A., Zhang, Y., Fang, J.K., Wu, C., Lam, P.K., 2021. Understanding Plastic Degradation and Microplastic Formation in the Environment: A Review. *Environmental Pollution*, 116554.
- Zhou, Y., Yang, Y., Liu, G., He, G., Liu, W., 2020. Adsorption mechanism of cadmium on microplastics and their desorption behavior in sediment and gut environments: the roles of water pH, lead ions, natural organic matter and phenanthrene. *Water Res.* 184, 116209.